Squeezing effect on three-dimensional Hanbury Brown-Twiss radii*

Yong Zhang (张勇)[1†] Peng Ru (茹芃)[2]

[1]School of Mathematics and Physics, Jiangsu University of Technology, Changzhou 213001, China
[2]School of Materials and New Energy, South China Normal University, Shanwei 516699, China

Abstract: This study examines the impact of the squeezing effect caused by the in-medium mass modification of particles on the three-dimensional Hanbury Brown-Twiss (HBT) radii. An analysis is conducted on how the squeezing effect impacts the three-dimensional HBT radii of $\phi\phi$, D^0D^0, and K^+K^+. The squeezing effect suppresses the impact of transverse flow on the transverse source distribution and broadens the space-time rapidity distribution of the particle-emitting source, leading to an increase in the HBT radii, particularly in the out and longitudinal directions. This phenomenon becomes more significant for higher transverse pair momentum, resulting in a non-monotonic decrease in the HBT radii with increasing transverse pair momentum. The impact of the squeezing effect on the HBT radii is more pronounced for D^0D^0 than for $\phi\phi$. Furthermore, this effect is also more significant for $\phi\phi$ than for K^+K^+. The findings presented in this paper could offer fresh perspectives on investigating the squeezing effect.

Keywords: squeezing effect, in-medium mass modification, HBT radii, $\phi\phi$, D^0D^0, K^+K^+

DOI: 10.1088/1674-1137/ade4a8 **CSTR:** 32044.14.ChinesePhysicsC.49114102

I. INTRODUCTION

The Hanbury Brown-Twiss (HBT) correlation, commonly referred to as the Bose-Einstein correlation, has become an important observable for investigating the spatial and temporal structure of particle-emitting sources created in relativistic heavy-ion collisions [1−6]. HBT radii are key parameters in HBT analyses that provide insights into the spatial and temporal dimensions of sources.

Because of their interactions with source media, the mass of the particles in the medium may vary from their vacuum mass. This variation can result in a squeezing effect, leading to an experimental observable known as squeezed back-to-back correlation (SBBC) between bosons and antibosons [7−16]. For sources that have a broad temporal distribution, the SBBC may be completely suppressed [10, 13]. Consequently, even with the squeezing effect, SBBC cannot provide feedback for sources with a broad temporal distribution. The squeezing effect influences the HBT correlation by reducing the impact of flow [10, 16], leading to a non-flow behavior in the one-dimensional HBT radii. Even for sources with broad temporal distributions, this non-flow behavior persists in the HBT radii [16]. Thus, the non-flow behavior of the HBT radii offers a new way to study squeezing effects beyond SBBC. Previous research on the influences of the squeezing effect on HBT was based on the spherically symmetric Gaussian expanding source [10, 16]. In fact, the sources formed in relativistic heavy-ion collisions are not spherically symmetric. In addition, one-dimensional HBT radii can not provide detailed information for each dimension. Hence, the impact of the squeezing effect on three-dimensional HBT radii must be studied further.

In this study, a locally thermalized cylinder expansion source [17, 18] is used to study the influences of the squeezing effect on three-dimensional HBT radii. The squeezing effect on the three-dimensional HBT radii of $\phi\phi$ and D^0D^0 is shown. The impact of the squeezing effect is more pronounced for the heavier bosons, which significantly influences the HBT results [16]. In addition, owing to their electrically neutral nature, ϕ and D^0 are not influenced by the Coulomb effect, making them better probes than charged bosons for investigating the squeezing effect.

Currently, there are no HBT experimental measurements for $\phi\phi$ and D^0D^0. Most experiments are for HBT measurements and analysis involving two pions and two kaons [19−30]. Owing to their higher mass, kaons may serve as a more effective probe for studying the squeezing effect in HBT radii compared to pions. Thus, we also investigate the impact of the squeezing effect on the three-dimensional HBT radii of K^+K^+. In the calculations, the Coulomb effect is not considered.

The squeezing effect affects the HBT radii by sup-

Received 22 March 2025; Accepted 9 June 2025; Published online 10 June 2025
* Supported by the National Natural Science Foundation of China (11905085), Guangdong Basic and Applied Basic Research Foundation (2022A1515110392)
† E-mail: zhy913@jsut.edu.cn

pressing the influence of transverse flow on the transverse source distribution and increasing the width of the space-time rapidity distribution of the particle-emitting source, ultimately increasing the HBT radii, particularly for large transverse pair momentum K_T. Consequently, the HBT radii no longer decreases monotonically with K_T. This phenomenon is referred to as the non-flow behavior of the HBT radii [16]. This strange HBT radii behavior may offer new insights into the study of squeezing effects. The squeezing effect has a more significant impact on R_o and R_l than R_s. The impact of the squeezing effect on HBT radii is enhanced for bosons with larger masses and at lower freeze-out temperatures.

The ϕ, D, and kaon mesons serve as excellent probes for investigating the quark-gluon plasma (QGP) generated during relativistic heavy-ion collisions because they contain either a strange or a charm quark, which are known to experience the complete QGP evolution resulting from these collisions. A great deal of attention has been triggered by the latest investigations into experimental data related to the ϕ, D, and kaon mesons [31−65]. In addition, it was anticipated that the interactions with the medium would induce modifications to the masses of ϕ, D, and kaon mesons within the particle-emitting sources produced during relativistic heavy-ion collisions [66−75]. Consequently, the analysis presented in this paper applies to relativistic heavy-ion collisions.

The rest of the paper is organized as follows: Section II presents the equations of the HBT correlation function with the squeezing effect for cylinder expansion sources. Additionally, this section presents the formulas of the three-dimensional HBT radii based on a Gaussian form. Section III examines the impact of the squeezing effect on the distributions of sources for the ϕ, D^0, and K^+ mesons. It also analyzes how the squeezing effect influences the three-dimensional HBT radii of $\phi\phi$, D^0D^0, and K^+K^+. Finally, Sec. IV concludes the paper with a summary and discussion.

II. FORMULAS

The HBT correlation function of two identical bosons was defined as [1−6]

$$C(\mathbf{q},\mathbf{K}) = 1+\frac{\left|\int \mathrm{d}^4 r S(r,K)\mathrm{e}^{\mathrm{i}q\cdot r}\right|^2}{\int \mathrm{d}^4 r S(r,k_1)\mathrm{d}^4 r S(r,k_2)}. \tag{1}$$

$S(r,k)$ denotes the emission function. The momenta of the two bosons are denoted by k_1 and k_2, respectively. Additionally, $\mathbf{q}=\mathbf{k}_1-\mathbf{k}_2$ and $\mathbf{K}=(\mathbf{k}_1+\mathbf{k}_2)/2$ are the relative and pair momentum of two identical bosons. For cylinder expansion sources, the emission function can be represented as [17, 18]

$$S(r,k) = M_T\cosh(\eta-Y)f(r,k) \times\exp\left(-\frac{r_T^2}{2R_g^2}-\frac{\eta^2}{2(\delta\eta)^2}\right)\delta(\tau-\tau_0). \tag{2}$$

Here, $M_T=\sqrt{m^2+k_T^2}$ is the transverse mass, where m and $k_T=\sqrt{k_x^2+k_y^2}$ are the mass and the transverse momentum of boson in a vacuum, respectively. Y is the rapidity of the boson. $r_T=\sqrt{x^2+y^2}$ and $\eta=\frac{1}{2}\ln[(t+z)/(t-z)]$ are the transverse coordinate and the space-time rapidity, respectively. R_g and $\delta\eta$ are the parameters that govern the width of the transverse distribution and the width of the space-time rapidity distribution, respectively. $\tau=\sqrt{t^2-z^2}$ is the proper time. In this study, it is assumed that the bosons freeze-out at a constant proper time τ_0. $f(r,k)$ is the momentum distribution of the bosons at the freeze-out point r. When the squeezing effect is not taken into account, the boson $f(r,k)$ is [17, 18]

$$f(r,k)=\frac{1}{\exp[k^\mu u_\mu(r)/T]-1}. \tag{3}$$

$k^\mu=(E_\mathbf{k}=\sqrt{\mathbf{k}^2+m^2},\mathbf{k})$ is the four-momentum of the boson. T is the freeze-out temperature of the boson. $u_\mu(r)$ is the four-velocity, which was assumed as [17, 18]

$$u_\mu(r)=(\cosh\eta\cosh\eta_T,\sinh\eta_T\vec{e}_T,\sinh\eta\cosh\eta_T), \tag{4}$$

Here, $\vec{e}_T=(x/r_T,y/r_T)$. The transverse flow rapidity, denoted as η_T, is defined as [18]

$$\begin{cases}\eta_T=\eta_{T\max}\dfrac{r_T}{R_G} & r_T<R_G,\\ \eta_T=\eta_{T\max} & r_T\geq R_G.\end{cases} \tag{5}$$

The value of $\eta_{T\max}$ is calculated using $\eta_{T\max}=\frac{1}{2}\ln\left(\frac{1+\beta}{1-\beta}\right)$, where β is a parameter.

When the squeezing effect is considered, $f(r,k)$ becomes [1−10, 16]

$$f(r,k)=|c_{\mathbf{k}'}|^2 n_{\mathbf{k}'}+|s_{-\mathbf{k}'}|^2(n_{-\mathbf{k}'}+1), \tag{6}$$

$$c_{\mathbf{k}'}=\cosh[r_{\mathbf{k}'}],\ s_{\mathbf{k}'}=\sinh[r_{\mathbf{k}'}], \tag{7}$$

$$r_{\mathbf{k}'}=\frac{1}{2}\log[E_{\mathbf{k}'}/\varepsilon_{\mathbf{k}'}], \tag{8}$$

$$E_{\mathbf{k}'}(r)=\sqrt{\mathbf{k}'^2(r)+m^2}=k^\mu u_\mu(r), \tag{9}$$

$$\varepsilon_{\mathbf{k}'}(r) = \sqrt{\mathbf{k}'^2(r)+m_*^2} = \sqrt{[E_{\mathbf{k}'}(r)]^2-m^2+m_*^2}, \tag{10}$$

$$n_{\mathbf{k}'} = \frac{1}{\exp(\varepsilon_{\mathbf{k}'}(r)/T)-1}. \tag{11}$$

Here, $\mathbf{k}'$ denotes the local-frame momentum corresponding to $\mathbf{k}$, while m_* refers to the mass of the boson in the source medium. When $m_* = m$, it means there is no change in mass in the medium, causing $f(r,k)$ in Eq. (6) to be equal to $f(r,k)$ in Eq. (3). This condition, where $m_* = m$, also implies that the squeezing effect is not considered in the calculations.

The Gaussian form of the HBT correlation function can be expressed as [18]:

$$C(\mathbf{q},\mathbf{K}) = 1+\lambda\exp[-q_o^2R_o^2(\mathbf{K})-q_s^2R_s^2(\mathbf{K})-q_l^2R_l^2(\mathbf{K})], \tag{12}$$

Here, λ represents the coherence parameter. q_l is the spatial component of $\mathbf{q}$ in the beam direction ("longitudinal" direction), while q_o and q_s are the spatial components of $\mathbf{q}$ parallel to the transverse component $\mathbf{K}_T$ of $\mathbf{K}$ ("out" direction) and perpendicular to the transverse component $\mathbf{K}_T$ ("side" direction), respectively. R_o^2, R_s^2, and R_l^2 were expressed as [17, 18]

$$R_o^2 = \langle(r_o-\beta_o t)^2\rangle - \langle r_o-\beta_o t\rangle^2, \tag{13}$$

$$R_s^2 = \langle r_s^2\rangle, \tag{14}$$

$$R_l^2 = \langle(r_l-\beta_l t)^2\rangle - \langle r_l-\beta_l t\rangle^2, \tag{15}$$

$$\beta_i = \frac{2K_i}{E_1+E_2} \approx \frac{K_i}{E_K}. \tag{16}$$

Here, the average notation is defined as

$$\langle\zeta\rangle = \frac{\int \mathrm{d}^4 r\zeta S(r,K)}{\int \mathrm{d}^4 r S(r,K)}. \tag{17}$$

III. RESULTS

In this section, the impact of the squeezing effect on the three-dimensional HBT radii of $\phi\phi$, D^0D^0, and K^+K^+ is shown. In the calculations, the parameters R_G and $\delta\eta$ are considered to be 6 fm and 3.0 [18], respectively, representing the transverse width and the space-time rapidity width of the source. The parameter τ_0 is taken to be 10 fm/c [18]. The transverse expansion velocity of the source is determined by the parameter β and is set to 0, 0.3, and 0.5.

The masses of the particles ϕ, D^0, and K^+ in a vacuum, represented by m, are known to be 1.01946 GeV, 1.86484 GeV, and 0.49368 GeV [76], respectively. The mass modification in a medium is represented by δm, where $\delta m = m - m_*$. If $\delta m = 0$, this indicates that the squeezing effect is not considered in the calculations. In the pionic medium, it is anticipated that the masses of the particles ϕ, D^0, and K^+ will decrease [66, 70]. Thus, δm is assumed to be greater than 0. The freeze-out temperature for the ϕ meson is considered to be 0.14 GeV [9, 16], with a comparative analysis performed for 0.15 GeV. The freeze-out temperature for the D^0 meson is set to 0.14 GeV and 0.15 GeV, and the freeze-out temperature for the K^+ meson is similarly set to 0.14 GeV and 0.15 GeV. The rapidity Y is considered to be within the range of $(-1,1)$, except in the longitudinally co-moving system (LCMS) shown in Figs. 3, 7, and 11. In the LCMS, $Y = 0$ [3, 17].

A. $\phi\phi$

In Fig. 1, the normalized distributions of the transverse coordinate of the ϕ emission sources are shown for k_T values of 0.5 GeV and 1.5 GeV. Here, $T = 0.14$ GeV in plots (a) and (b) and $T = 0.15$ GeV in plots (c) and (d). $\beta = 0$ indicates that velocity expansion is absent in the transverse plane and that the transverse source distributions for k_T = 1.5 GeV are identical to those for k_T = 0.5 GeV. When the squeezing effect is not considered ($\delta m = 0$), the transverse flow leads to a shift in the transverse source distributions for k_T = 0.5 GeV toward a smaller transverse coordinate r_T. However, in the transverse source distributions for k_T = 1.5 GeV, it leads to a shift toward a larger transverse coordinate r_T. This occurs because particles with low transverse momentum are more likely to be produced in greater quantities at lower transverse velocities, while locations with higher transverse velocities tend to generate more high transverse momentum particles. In the model discussed in this paper, the transverse flow increases as the transverse coordinate r_T increases. With the increase in transverse velocity, this phenomenon becomes more pronounced. This phenomenon is slighlty more pronounced for $T = 0.14$ GeV than for $T = 0.15$ GeV. The mass of the ϕ meson is expected to decrease around 0.01 GeV in the pionic medium [70]. When considering the squeezing effect, the δm for a ϕ meson is taken as 0.01 GeV, as in Figs. 1−3. For $\beta = 0$, the squeezing effect does not affect the transverse source distribution. However, for $\beta > 0$, the squeezing effect reduces the influence of transverse flow on the transverse source distribution at k_T = 1.5 GeV while having no impact at k_T = 0.5 GeV. This phenomenon is more pronounced for $T = 0.14$ GeV.

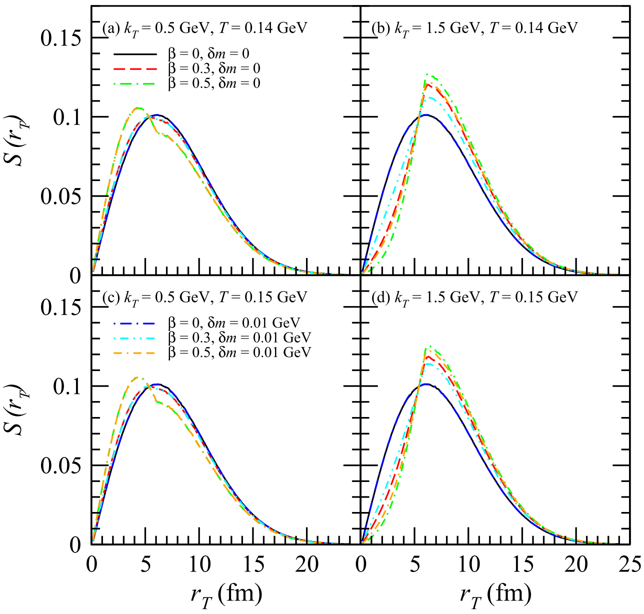

Fig. 1. (color online) Normalized distributions of the transverse coordinate of the ϕ emission sources for k_T = 0.5 GeV and 1.5 GeV. Here, T = 0.14 GeV in plots (a) and (b) and T = 0.15 GeV in plots (c) and (d).

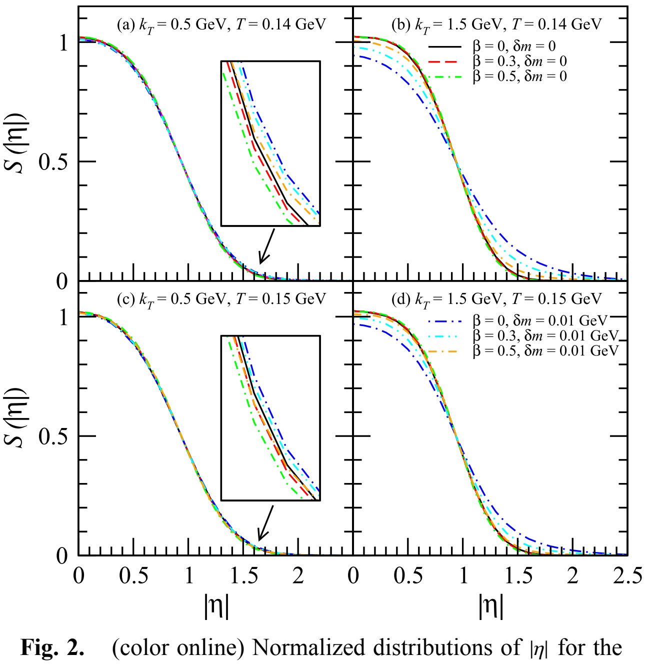

Fig. 2. (color online) Normalized distributions of $|\eta|$ for the ϕ emission sources at k_T = 0.5 GeV and 1.5 GeV.

In Fig. 2, the normalized distributions of $|\eta|$ for the ϕ emission sources for k_T = 0.5 GeV and 1.5 GeV are shown. Here, η is the space-time rapidity. For $\delta m = 0$, the transverse flow reduces both the width of the temporal distribution and the width of the longitudinal distribution of the sources. The squeezing effect leads to the widening of the source space-time rapidity distribution, which is more obvious for k_T = 1.5 GeV. This phenomenon is more pronounced for lower transverse flow or smaller freeze-out temperatures.

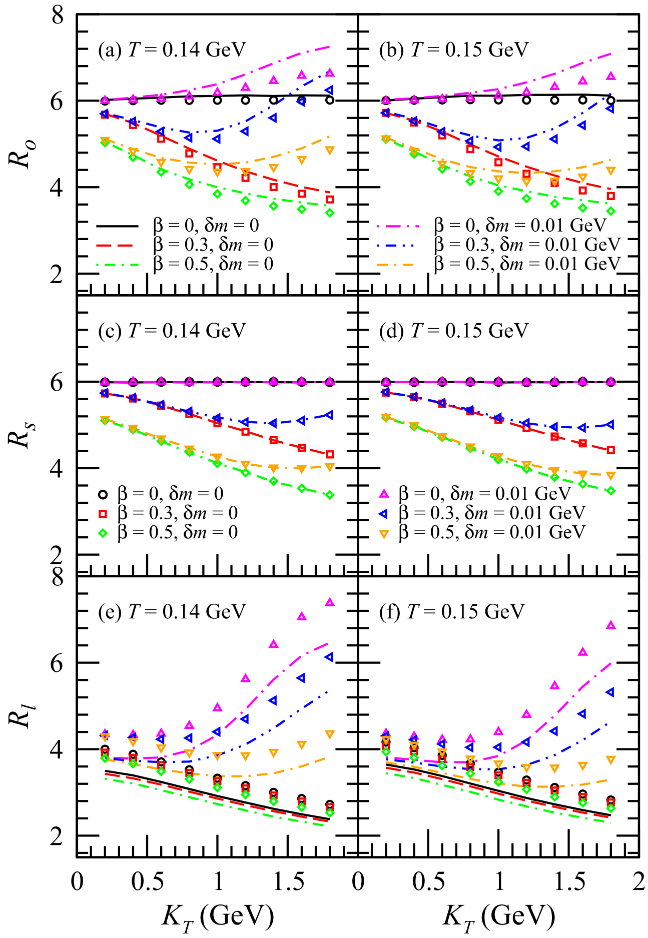

Fig. 3. (color online) HBT radii R_o, R_s, and R_l of $\phi\phi$ with respect to the transverse pair momentum K_T. The plots illustrate the results of R_o in (a) and (b), R_s in (c) and (d), and R_l in (e) and (f). The lines represent the results for Y within the range of $(-1,1)$, while the symbols denote the results calculated in the LCMS.

For the discussed model, $t=\tau\cosh\eta$ and $z=\tau\sinh\eta$. Therefore, by reducing the width of the source space-time rapidity distribution, the transverse flow reduces the width of the temporal distribution of the longitudinal distribution. However, the squeezing effect leads to the widening of the source space-time rapidity distribution, which results in an expansion of both the temporal distribution and the longitudinal distribution of the source.

Figure 3 shows the HBT radii R_o, R_s, and R_l of $\phi\phi$ with respect to the transverse pair momentum K_T. The plots illustrate the results of R_o in (a) and (b), R_s in (c) and (d), and R_l in (e) and (f). The lines represent the results for Y within the range $(-1,1)$, while the symbols denote the results calculated in the LCMS. In this paragraph, the results for Y in the range $(-1,1)$ are discussed first, followed by a discussion of the differences between these results and those obtained in the LCMS. The value of R_o is related to the temporal and transverse spatial distribution of the source. When the squeezing effect is not considered ($\delta m = 0$), the transverse flow causes a reduction in the transverse spatial distribution width, particularly for large K_T (see Fig. 1). Furthermore, the transverse flow slightly diminishes the width of the source space-time rapidity distribution (see Fig. 2), leading to a decrease in the width of the source temporal distribution. Therefore, under the influence of the transverse flow, R_o decreases as K_T increases for $\beta > 0$. The squeezing effect reduces the influence of transverse flow on the transverse source distribution for large k_T (see Fig. 1 (b) and (d)) while having no impact for small k_T (see Fig. 1 (a) and (c)). Moreover, the squeezing effect results in the widening of the source space-time rapidity distribution, consequently expanding the temporal distribution of the source, particularly for large k_T (see Fig. 2). As a result, the squeezing effect leads to an increase in R_o, which is more pronounced at high K_T values. The value of R_s is only related to the transverse spatial distribution of the source. When $\beta = 0$, the squeezing effect has no impact on the transverse source distribution (see Fig. 1), thus not influencing R_s either. For $\beta > 0$, the squeezing effect leads to an increase in R_s, which is more pronounced at high K_T values. This outcome is due to the impact of the squeezing effect on the transverse source distribution. The value of R_l is related to the temporal and longitudinal spatial distribution of the source. The squeezing effect leads to the widening of the source space-time rapidity distribution, which results in an expansion of both the temporal distribution and the longitudinal distribution of the source. These effects are more pronounced for large k_T. Hence, the squeezing effect leads to an increase in R_l, which is more pronounced at high K_T values. The squeezing effect has a more significant impact on R_o and R_l than R_s. The squeezing effect has a slightly greater impact on R_o, R_s, and R_l at $T = 0.14$ GeV compared to $T = 0.15$ GeV. R_o, R_s, and R_l no longer monotonically decreasing with increasing K_T because the squeezing effect is more pronounced at high K_T is called the non-flow behavior of the HBT radii [16]. The R_o calculated in the LCMS is slightly lower than that calculated for Y in the range $(-1,1)$. Conversely, the R_s calculated in the LCMS is the same as that calculated for Y in the range $(-1,1)$. However, the R_l calculated in the LCMS is greater than that calculated for Y in the range $(-1,1)$. The impact of the squeezing effect on the HBT radii in the LCMS is similar to its impact on the HBT radii for Y in the range $(-1,1)$. When accounting for the squeezing effect, the difference between the values of R_o and R_l calculated in the LCMS and the values of R_o and R_l for Y within the range $(-1,1)$ is greater than the difference observed without the squeezing effect.

Figure 4 shows the HBT radii R_o, R_s, and R_l of $\phi\phi$ with respect to the in-medium mass modification δm for K_T = 0.5 GeV and 1.5 GeV. When $\beta = 0$, the squeezing effect does not affect R_s, which remains constant as δm increases. However, in other instances, as δm increases, the values of R_o, R_s, and R_l increase before they reach a plateau, indicating a decreasing slope for the relationship between R_o, R_s, and R_l and δm. Ultimately, R_o, R_s, and R_l stabilize with minimal changes as δm increases. When $\delta m < 0.02$ GeV, the slopes of the functions of R_o, R_s, and R_l versus δm are significantly larger at K_T = 1.5 GeV than at K_T = 0.5 GeV, and they are slightly larger at T = 0.14 GeV than at T = 0.15 GeV.

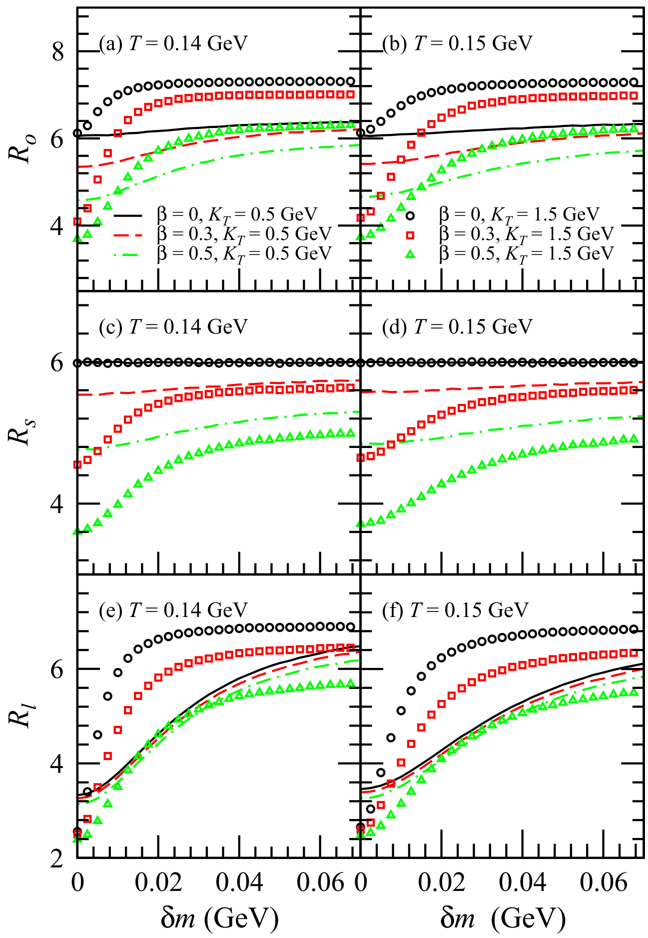

Fig. 4. (color online) HBT radii R_o, R_s, and R_l of $\phi\phi$ with respect to the in-medium mass modification δm for K_T = 0.5 GeV and 1.5 GeV. The plots illustrate the results of R_o in (a) and (b), R_s in (c) and (d), and R_l in (e) and (f).

B. $D^0 D^0$

Figure 5 shows the normalized distributions of the transverse coordinate of the D^0 emission sources for k_T = 0.5 GeV and 1.5 GeV. Here, T = 0.14 GeV in plots (a) and (b) and T = 0.15 GeV in plots (c) and (d). For $\beta = 0$, it indicates that velocity expansion is absent in the transverse plane and that the transverse source distributions

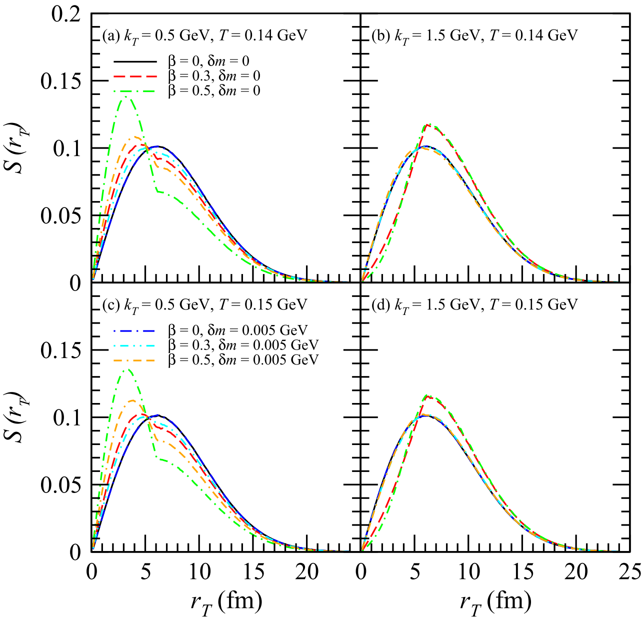

Fig. 5. (color online) Normalized distributions of the transverse coordinate of the D^0 emission sources for k_T = 0.5 GeV and 1.5 GeV. Here, T = 0.14 GeV in plots (a) and (b) and T = 0.15 GeV in plots (c) and (d).

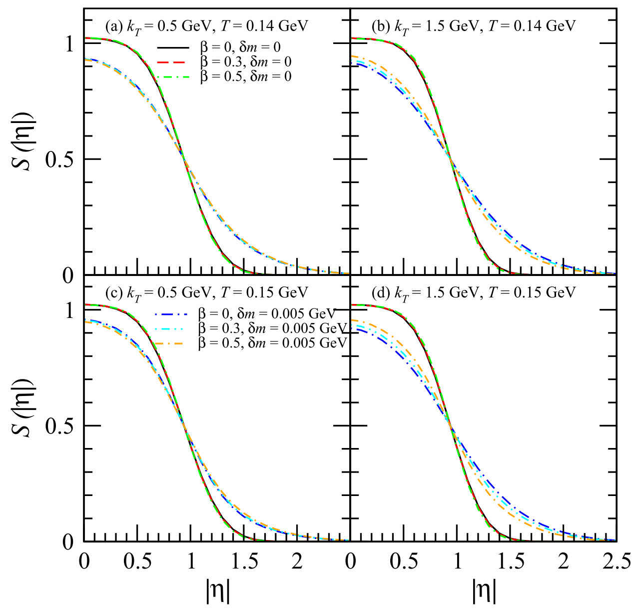

Fig. 6. (color online) Normalized distributions of $|\eta|$ of the D^0 emission sources for k_T = 0.5 GeV and 1.5 GeV.

for k_T = 1.5 GeV are identical to those for k_T = 0.5 GeV. When the squeezing effect is not considered ($\delta m = 0$), the transverse flow shifts the transverse source distributions for k_T= 0.5 GeV toward a smaller transverse coordinate r_T and shifts the transverse source distributions for k_T= 1.5 GeV toward a larger transverse coordinate r_T. The mass of the D^0 meson is expected to be reduced by approximately 0.005 GeV in the pionic medium [66]. When considering the squeezing effect, the δm for the D^0 meson is taken as 0.005 GeV, as in Figs. 5−7. For $\beta = 0$, the squeezing effect does not affect the transverse source distribution. However, for $\beta > 0$, the squeezing effect reduces the influence of the transverse flow on the transverse source distribution, which is more pronounced for k_T = 1.5 GeV. This phenomenon is slightly more pronounced for T = 0.14 GeV. The squeezing effect affects the transverse source distribution of the D^0 meson to a greater extent than for the ϕ meson.

Figure 6 shows the normalized distributions of $|\eta|$ of the D^0 emission sources for k_T= 0.5 GeV and 1.5 GeV. The squeezing effect results in the widening of the distribution of $|\eta|$ of the D^0 emission sources, which is more pronounced for k_T = 1.5 GeV. This phenomenon is slightly more pronounced for T = 0.14 GeV.

Figure 7 shows the HBT radii R_o, R_s, and R_l of D^0D^0 with respect to the transverse pair momentum K_T. The lines represent the results for Y within the range $(-1,1)$, while the symbols denote the results calculated in the LCMS. In this paragraph, the results for Y in the range $(-1,1)$ are discussed first, followed by a discussion of the

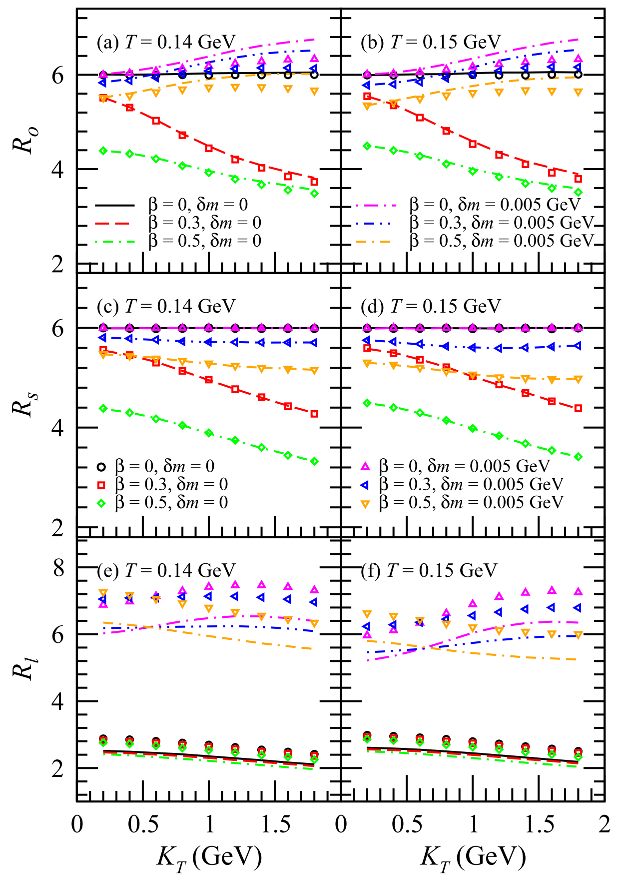

Fig. 7. (color online) HBT radii R_o, R_s, and R_l of D^0D^0 with respect to the transverse pair momentum K_T. The plots illustrate the results of R_o in (a) and (b), R_s in (c) and (d), and R_l in (e) and (f). The lines represent the results for Y within the range of $(-1,1)$, while the symbols denote the results calculated in the LCMS.

differences between these results and those obtained in the LCMS. The squeezing effect leads to an increase in R_o, which is more pronounced at high K_T values. This is due to the impact of the squeezing effect on the source distribution. For $\beta = 0$, the squeezing effect does not affect the transverse source distribution. The value of R_s solely depends on the transverse spatial distribution of the source. Hence, at $\beta = 0$, the squeezing effect has no bearing on the value of R_s. For $\beta > 0$, the squeezing effect leads to an increase in R_s, which is slightly more pronounced at high K_T values. The squeezing effect results in a significant increase in R_l. This is because the squeezing effect causes a significant widening of the source space-time rapidity distribution, leading to an expansion of both the temporal and longitudinal distributions of the source. The squeezing effect has a slightly greater impact on the R_o, R_s, and R_l of D^0D^0 at $T = 0.14$ GeV than at $T = 0.15$ GeV. The value of R_o calculated in the LCMS is slightly lower than that calculated for Y within the range $(-1, 1)$, while the value of R_l calculated in the LCMS exceeds that calculated for Y in the range $(-1, 1)$. When considering the squeezing effect, this difference becomes more pronounced compared to when it is not considered. In contrast, the value of R_s calculated in the LCMS is identical to that calculated for Y in the range $(-1, 1)$. The influence of the squeezing effect on the HBT radii of D^0D^0 in the LCMS closely resembles its influence on the HBT radii of D^0D^0 for Y in the range $(-1, 1)$.

Figure 8 presents the HBT radii R_o, R_s, and R_l of D^0D^0 with respect to δm for K_T = 0.5 GeV and 1.5 GeV. When $\beta = 0$, the squeezing effect has no impact on R_s, which remains steady as δm increases. However, in other instances, as δm increases, the values of R_o, R_s, and R_l initially increase before leveling off, presenting a decreasing slope in the relationship between R_o, R_s, and R_l and δm. Eventually, R_o, R_s, and R_l stabilize with no changes as δm increases further.

The squeezing effect exerts a greater influence on the values of R_o, R_s, and R_l of D^0D^0 compared to $\phi\phi$ because the mass of D^0 is greater than that of ϕ. The squeezing effect significantly influences the three-dimensional HBT radii, particularly R_o and R_l, for cylinder expansion sources compared to the one-dimensional HBT radii for spherically symmetric sources. This is due to the notable impact of this effect on the source space-time rapidity distribution in cylinder expansion sources.

C. K^+K^+

Figure 9 shows the normalized distributions of the transverse coordinate of the K^+ emission sources for k_T= 0.5 GeV and 1.5 GeV. In the figure, T = 0.14 GeV in (a) and (b) and T = 0.15 GeV in (c) and (d). For $\beta = 0$, it indicates the absence of any velocity expansion in the transverse plane, with the transverse source distributions for k_T = 1.5 GeV being identical to those for k_T = 0.5 GeV.

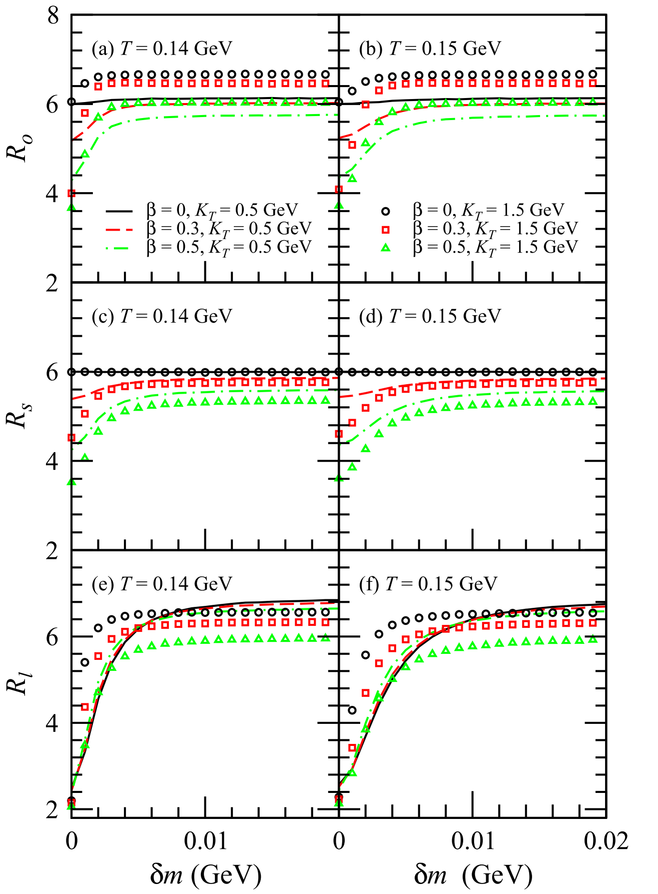

Fig. 8. (color online) HBT radii R_o, R_s, and R_l of D^0D^0 with respect to δm for K_T = 0.5 GeV and 1.5 GeV. The plots illustrate the results of R_o in (a) and (b), R_s in (c) and (d), and R_l in (e) and (f).

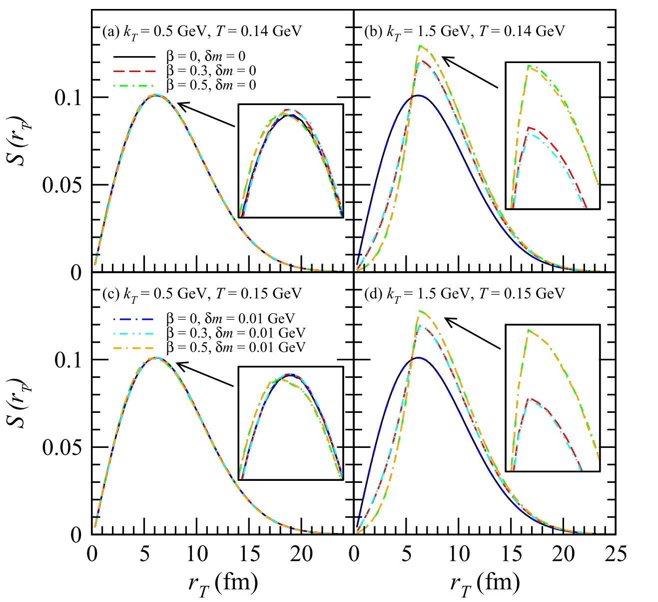

Fig. 9. (color online) Normalized distributions of the transverse coordinate of the K^+ emission sources for k_T = 0.5 GeV and 1.5 GeV. Here, T = 0.14 GeV in (a) and (b) and T = 0.15 GeV in (c) and (d).

When the squeezing effect is not considered ($\delta m = 0$), the transverse flow has a slight influence on the transverse source distributions at k_T = 0.5 GeV. For $\beta = 0.3$, the transverse flow induces a slight shift in these distributions toward larger transverse coordinates r_T at k_T = 0.5 GeV. Conversely, at $\beta = 0.5$, the transverse flow causes a slight shift in the transverse source distributions toward a smaller transverse coordinate r_T for k_T = 0.5 GeV. This occurs because, at $\beta = 0.3$, the transverse flow within regions of small transverse coordinates r_T is low, resulting in less K^+ particle production with k_T= 0.5 GeV. The transverse flow induces a shift in the transverse source distributions toward larger transverse coordinates r_T at k_T = 1.5 GeV. As the transverse flow increases, this phenomenon becomes more pronounced. At T = 0.14 GeV, this phenomenon is slightly more significant than at T = 0.15 GeV. The mass of Kaon is expected to be reduced by approximately 0.01 GeV in the pionic medium [70]. When considering the squeezing effect, the δm for K^+ is taken as 0.01 GeV, as in Figs. 9−11. For $\beta = 0$, the squeezing effect does not impact the transverse source distribution. However, for $\beta > 0$, the squeezing effect slightly decreases the influence of transverse flow on the transverse source distribution at k_T = 1.5 GeV while having no impact at k_T = 0.5 GeV. This phenomenon is more pronounced for T = 0.14 GeV.

Figure 10 shows the normalized distributions of $|\eta|$ for the K^+ emission sources for k_T = 0.5 GeV and 1.5 GeV. For $\delta m = 0$, the transverse flow slightly reduces the effect on the space-time rapidity distribution of the sources. At k_T= 0.5 GeV, the squeezing effect does not influence the source's space-time rapidity distribution. However, at k_T = 1.5 GeV, the squeezing effect causes a slight expansion of the source's space-time rapidity distribution. This phenomenon is more pronounced with lower transverse flow and smaller freeze-out temperatures.

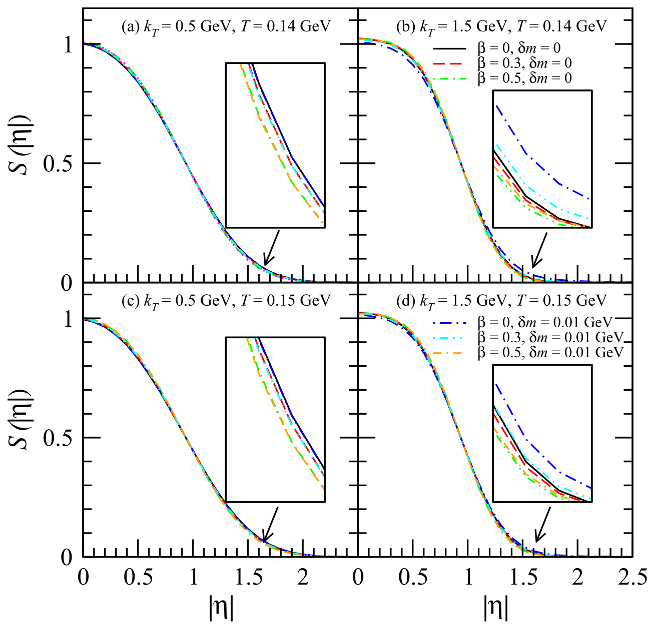

Fig. 10. (color online) Normalized distributions of $|\eta|$ of the K^+ emission sources for k_T = 0.5 GeV and 1.5 GeV.

Figure 11 shows the HBT radii R_o, R_s, and R_l of K^+K^+ with respect to the transverse pair momentum K_T. Here, the lines represent the results for Y within the range $(-1,1)$, while the symbols denote the results calculated in the LCMS. At high values of K_T, the squeezing effect results in an increase in both R_o and R_l. The increase in R_l is more significant than that in R_o. This phenomenon is more obvious for larger K_T, as well as for lower transverse flow and freeze-out temperatures. This is due to the influences of the squeezing effect on the source distribution. For $\beta = 0$, the squeezing effect does not affect the transverse source distribution; hence, it also has no impact on R_s. For $\beta > 0$, the squeezing effect leads to a slight increase in R_s at high K_T. The R_s calculated in the LCMS is identical to that calculated for Y in the range $(-1,1)$. The R_o calculated in the LCMS is slightly lower

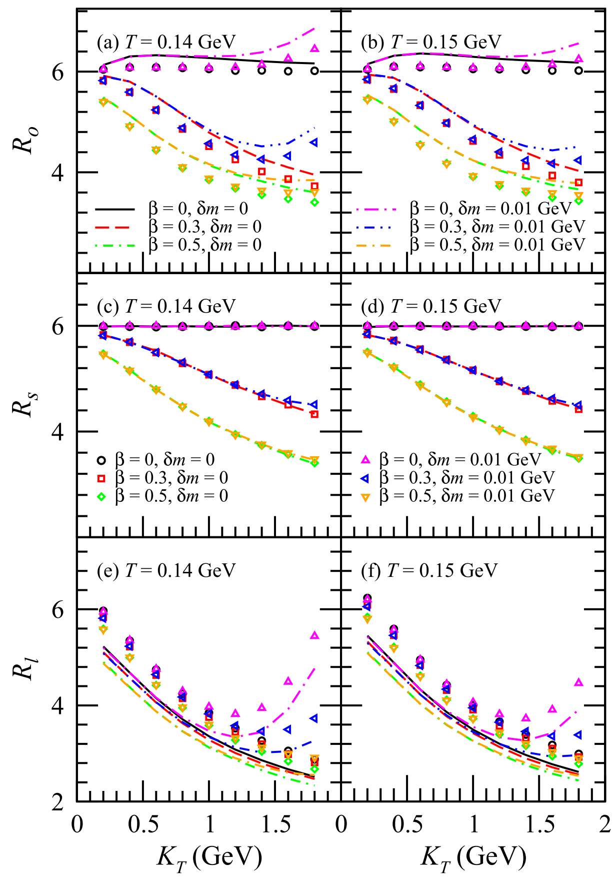

Fig. 11. (color online) HBT radii R_o, R_s, and R_l of K^+K^+ with respect to the transverse pair momentum K_T. The plots illustrate the results of R_o in (a) and (b), R_s in (c) and (d), and R_l in (e) and (f). The lines represent the results for Y within the range of $(-1,1)$, while the symbols denote the results calculated in the LCMS.

than that calculated for Y in the range $(-1,1)$, while the R_l calculated in the LCMS is greater than that calculated for Y in the range $(-1,1)$. The squeezing effect's impact on the HBT radii of K^+K^+ in the LCMS is similar to the effect observed by Y in the range $(-1,1)$. For a small in-medium mass modification, the squeezing effect exerts a weaker influence on the HBT radii of K^+K^+ compared to $\phi\phi$ and D^0D^0, which can be attributed to the lower mass of K^+ relative to ϕ and D^0.

Figure 12 shows the HBT radii R_o, R_s, and R_l of K^+K^+ with respect to δm for $K_T = 0.5$ GeV and 1.5 GeV. For $\beta=0$, the squeezing effect does not influence R_s, which remains constant as δm increases. For $\beta>0$, as δm increases, R_s undergoes minimal changes when $K_T = 0.5$ GeV. However, in other instances, as δm increases, R_o, R_s, and R_l first increase monotonically before saturating, showing a decay in the slope of their correlation with δm. Ultimately, further increases in δm result in no significant changes to R_o, R_s, and R_l.

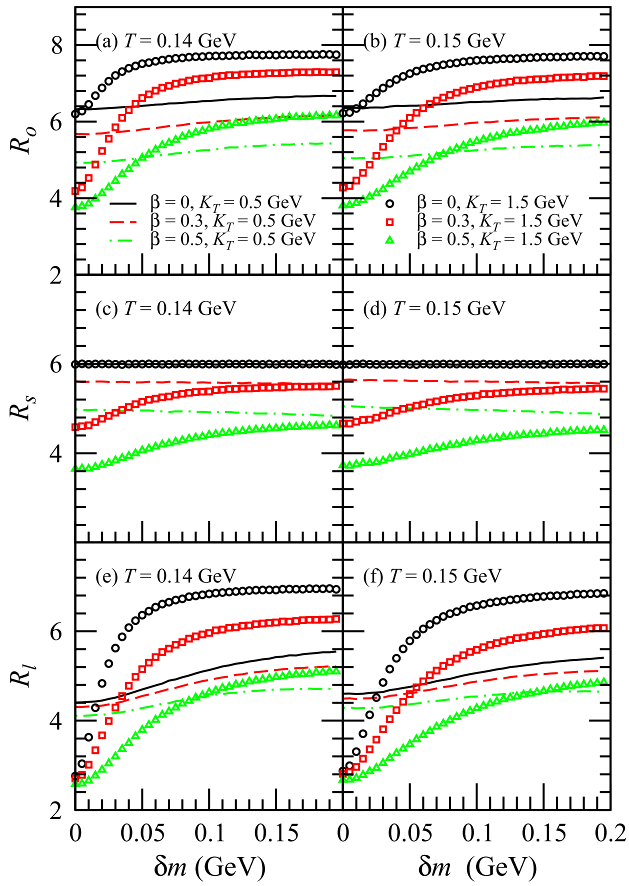

Fig. 12. (color online) HBT radii R_o, R_s, and R_l of K^+K^+ with respect to δm for $K_T = 0.5$ GeV and 1.5 GeV. The plots illustrate the results of R_o in (a) and (b), R_s in (c) and (d), and R_l in (e) and (f).

IV. SUMMARY AND DISCUSSION

Boson interactions with source media result in a shift in the masses of the bosons, inducing a squeezing effect. In this study, the impact of the squeezing effect on the three-dimensional HBT radii is analyzed based on cylinder expansion sources.

The impact of the squeezing effect on the three-dimensional HBT radii of $\phi\phi$, D^0D^0, and K^+K^+ is analyzed. The squeezing effect suppresses the impact of transverse flow on the transverse source distribution and broadens the space-time rapidity distribution of the source, increasing the HBT radii, particularly in the out and longitudinal directions. This phenomenon is more pronounced for a larger transverse pair momentum K_T. Consequently, the HBT radii do not monotonically decrease with increasing K_T. This phenomenon is referred to as the non-flow behavior of the HBT radii. The squeezing effect has a slightly greater impact on R_o, R_s, and R_l at $T=0.14$ GeV than at $T=0.15$ GeV, and it exerts a greater influence on the values of R_o, R_s, and R_l of D^0D^0 than those of $\phi\phi$. Additionally, the squeezing effect is more significant for $\phi\phi$ than for K^+K^+. The squeezing effect has a greater impact on the three-dimensional radii of the HBT, particularly R_o and R_l, for cylinder expansion sources than for one-dimensional radii for spherically symmetric sources.

The non-flow behavior of R_o and R_l for D^0D^0 and $\phi\phi$ can be better manifested in the small transverse momentum region than that of K^+K^+. The non-flow behavior of R_o and R_l for D^0D^0 and $\phi\phi$ may be more likely to be measured experimentally than that of K^+K^+. For small transverse flow, the squeezing effect has a more pronounced influence on the R_o and R_l of K^+K^+ than it does for large transverse flow. The non-flow behavior of R_o and R_l for K^+K^+ may be observed in the large transverse momentum region for small transverse flow. However, the current transverse momentum range used for measuring the HBT radii of K^+K^+ has not yet reached the region where this non-flow behavior occurs [25–30]. It should be emphasized that the effects demonstrated in this study manifest only when particles undergo in-medium mass modifications. In the absence of such mass modifications, the non-flow behavior signals of the HBT radii will be entirely absent.

In this study, the Gaussian form is used in the analysis of the three-dimensional HBT radii. Due to the squeezing effect, the distribution of the source may deviate from a Gaussian form. Studying the effects of the squeezing effect on the source's shape is valuable. For instance, this can be achieved by employing a Lévy-type form [77–80] to study how the squeezing effect influences both the three-dimensional HBT radii and the source's shape.

The cylinder expansion source used in this study is more reasonable compared to the previously utilized spherically symmetric source [16]. The independent transverse spatial distribution and temporal distribution of the cylinder expansion source differs from phyisical conditions. Investigating the influence of the squeezing effect on three-dimensional HBT radii through the utilization of more realistic sources, such as hydrodynamical sources, presents an interesting direction for further exploration.

References

[1] M. Gyulassy, S. K. Kauffmann, and Lance W. Wilson, Phys. Rev. C **20**, 2267 (1979)
[2] C. Y. Wong, *Introduction to High-Energy Heavy-Ion Collisions* (World Scientific, Singapore, 1994), Chap. 17
[3] U. A. Wienemann and U. Heinz, Phys. Rep. **319**, 145 (1999)
[4] R. M. Weiner, Phys. Rep. **327**, 249 (2000)
[5] T. Csörgő, arXiv: hep-ph/0001233
[6] M. A. Lisa, S. Pratt, R. Soltz *et al*., Annu. Rev. Nucl. Part. Sci. **55**, 357 (2005)
[7] M. Asakawa and T. Csörgő, Heavy Ion Physics **4**, 233 (1996)
[8] M. Asakawa, T. Csörgő, and M. Gyulassy, Phys. Rev. Lett. **83**, 4013 (1999)
[9] S. S. Padula, G. Krein, T. Csörgő *et al*., Phys. Rev. C **73**, 044906 (2006)
[10] D. M. Dudek and S. S. Padula, Phys. Rev. C **82**, 034905 (2010)
[11] Y. Zhang, J. Yang, and W. N. Zhang, Phys. Rev. C **92**, 024906 (2015)
[12] Y. Zhang, J. Yang, and W. N. Zhang, Chin. Phys. C **39**(3), 034103 (2015)
[13] Y. Zhang and W. N. Zhang, Eur. Phys. J. C **76**, 419 (2016)
[14] A. G. Yang, Y. Zhang, L. Cheng *et al*., Chin. Phys. Lett. **35**, 052501 (2018)
[15] P. Z. Xu, W. N. Zhang, and Y. Zhang, Phys. Rev. C **99**, 011902(R) (2019)
[16] Y. Zhang and P. Ru, Phys. Rev. C **109**, 024902 (2024)
[17] U. A. Wiedemann, P. Scotto, and U. Heinz, Phys. Rev. C **53**, 918 (1996)
[18] H. Yang, Q. C. Feng, Y. Y. Ren *et al*., Chin. Phys. C **44**(5), 054105 (2020)
[19] C. Adler *et al*. (STAR Collaboration), Phys. Rev. Lett. **87**, 082301 (2001)
[20] S. S. Adler *et al*. (PHENIX Collaboration), Phys. Rev. Lett. **93**, 152302 (2004)
[21] J. Adams *et al*. (STAR Collaboration), Phys. Rev. C **71**, 044906 (2005)
[22] B. Abelev *et al*. (ALICE Collaboration), Phys. Rev. C **89**, 024911 (2014)
[23] L. Adamczyk *et al*. (STAR Collaboration), Phys. Rev. C **92**, 014904 (2015)
[24] J. Adam *et al*. (ALICE Collaboration), Phys. Rev. C **93**, 024905 (2016)
[25] I. G. Bearden *et al*. (NA44 Collaboration), Phys. Rev. Lett. **87**, 112301 (2001)
[26] S. Afanasiev *et al*. (PHENIX Collaboration), Phys. Rev. Lett. **103**, 142301 (2009)
[27] A. Adare *et al*. (PHENIX Collaboration), Phys. Rev. C **92**, 034914 (2015)
[28] J. Adam *et al*. (ALICE Collaboration), Phys. Rev. C **92**, 054908 (2015)
[29] S. Acharya *et al*. (ALICE Collaboration), Phys. Rev. C **96**, 064613 (2017)
[30] S. Acharya *et al*. (ALICE Collaboration), Phys. Rev. C **100**, 024002 (2019)
[31] J. Adam *et al*. (STAR Collaboration), Phys. Rev. Lett. **127**, 092301 (2021)
[32] J. Adam *et al*. (STAR Collaboration), Phys. Rev. C **102**, 014905 (2020)
[33] J. Adam *et al*. (STAR Collaboration), Phys. Rev. C **99**, 034908 (2019)
[34] A. M. Sirunyan *et al*. (CMS Collaboration), Phys. Rev. Lett. **120**, 202301 (2018)
[35] A. M. Sirunyan *et al*. (CMS Collaboration), Phys. Lett. B **782**, 474 (2018)
[36] S. Acharya *et al*. (ALICE Collaboration), JHEP **2022**, 174 (2022)
[37] S. Acharya *et al*. (ALICE Collaboration), Eur. Phys. J. C **80**, 979 (2020)
[38] S. Acharya *et al*. (ALICE Collaboration), JHEP **2018**, 174 (2018)
[39] J. Adam *et al*. (ALICE Collaboration), JHEP **2016**, 081 (2016)
[40] J. Adam *et al*. (ALICE Collaboration), JHEP **2015**, 205 (2015)
[41] B. Abelev *et al*. (ALICE Collaboration), Phys. Rev. C **90**, 034904 (2014)
[42] B. Abelev *et al*. (ALICE Collaboration), Phys. Rev. Lett. **111**, 102301 (2013)
[43] S. Acharya *et al*. (ALICE Collaboration), Eur. Phys. J. C **83**, 540 (2023)
[44] S. Acharya *et al*. (ALICE Collaboration), Phys. Rev. C **106**, 034907 (2022)
[45] S. Acharya *et al*. (ALICE Collaboration), Eur. Phys. J. C **81**, 772 (2021)
[46] S. Acharya *et al*. (ALICE Collaboration), Eur. Phys. J. C **78**, 559 (2018)
[47] L. Adamczyk *et al*. (STAR Collaboration), Phys. Rev. Lett. **116**, 062301 (2016)
[48] L. Adamczyk *et al*. (STAR Collaboration), Phys. Rev. C **93**, 021903(R) (2016)
[49] A. Adare *et al*. (PHENIX Collaboration), Phys. Rev. C **93**, 024904 (2016)
[50] B. Abelev *et al*. (ALICE Collaboration), Phys. Rev. C **91**, 024609 (2015)
[51] A. Adare *et al*. (PHENIX Collaboration), Phys. Rev. C **83**, 024909 (2011)
[52] B. I. Abelev *et al*. (STAR Collaboration), Phys. Lett. B **673**, 183 (2009)
[53] B. I. Abelev *et al*. (STAR Collaboration), Phys. Rev. C **79**, 064903 (2009)
[54] B. I. Abelev *et al*. (STAR Collaboration), Phys. Rev. Lett. **99**, 112301 (2007)
[55] S. Afanasiev *et al*. (PHENIX Collaboration), Phys. Rev. Lett. **99**, 052301 (2007)
[56] S. S. Adler *et al*. (PHENIX Collaboration), Phys. Rev. C **72**, 014903 (2005)
[57] B. Alessandro *et al*. (NA50 Collaboration), Phys. Lett. B **555**, 147 (2003)
[58] C. Adler *et al*. (STAR Collaboration), Phys. Rev. C **65**,

041901(R) (2002)
[59] S. V. Afanasiev *et al*. (NA49 Collaboration), Phys. Lett. B **491**, 59 (2000)
[60] C. Adler *et al*. (STAR Collaboration), Phys. Lett. B **595**, 143 (2004)
[61] M. S. Abdallah *et al*. (STAR Collaboration), Phys. Rev. C **107**, 024901 (2023)
[62] T. Anticic *et al*. (NA49 Collaboration), Phys. Rev. C **86**, 054903 (2012)
[63] N. J. Abdulameer *et al*. (PHENIX Collaboration), Phys. Rev. C **109**, 054910 (2024)
[64] S. Acharya *et al*. (ALICE Collaboration), Phys. Rev. C **101**, 044907 (2020)
[65] S. Acharya *et al*. (ALICE Collaboration), Phys. Lett. B **832**, 137242 (2022)
[66] C. Fuchs, B. V. Martemyanov, A. Faessler *et al*., Phys. Rev. C **73**, 035204 (2006)
[67] G. Montaña, À. Ramos, L. Tolós *et al*., Phys. Lett. B **806**, 135464 (2020)
[68] R. Kumar, A. Kumar, Phys. Rev. C **101**, 015202 (2020)
[69] E. Braaten, R. Bruschini, L. P. He *et al*., Phys. Rev. D **108**, 076012 (2023)
[70] B.V. Martemyanov, A. Faessler, C. Fuchs *et al*., Phys. Rev. Lett. **93**, 052301 (2004)
[71] R. Kumar and A. Kumar, Phys. Rev. C **102**, 045206 (2020)
[72] H. Kim and P. Gubler, Phys. Lett. B **805**, 135412 (2020)
[73] M. Kaur and A. Kumar, Phys. Rev. D **110**, 114054 (2024)
[74] G. Gifari, P. T. P. Hutauruk, and T. Mart, Phys. Rev. D **110**, 014043 (2024)
[75] J. J. Cobos-Martínez, K. Tsushima, G. Krein *et al*., Phys. Lett. B **771**, 113 (2017)
[76] S.Navas *et al*. (Particle Data Group), Phys. Rev. D **110**, 030001 (2024)
[77] T. Csörgő, S. Hegyi, and W. A. Zajc, Eur. Phys. J. C **36**, 67 (2004)
[78] A. Adare *et al*. (PHENIX Collaboration), Phys. Rev. C **97**, 064911 (2018)
[79] H. Adhikary *et al*. (NA61/SHINE Collaboration), Eur. Phys. J. C **83**, 919 (2023)
[80] B. Kórodi, D. Kincses, and M. Csanád, Phys. Lett. B **847**, 138295 (2023)